2-photon ionization and necessary laser and vacuum systems for experiments with trapped strontium ions

E. Kirilov and S. Putterman
UCLA Department of Physics and Astronomy, Los Angeles, California 90095, USA

We describe a efficient way to photoionize strontium atoms in a linear radio-frequency trap. We use a 2-photon second order process to excite the autoionization resonance $(4d^2 + 5p^2)\ ^1D_2$. A doubled pulsed Ti:Saphire laser system is used at 431nm to provide 100fsec pulses at 82Mhz. The fabrication of the laser systems for addressing the Sr^+ transitions necessary for laser cooling and excitation of quantum jumps, vacuum system and ion trap structure are also described in detail. With the current setup a easy and repeatable trapping of linear ion chains is achieved at low $\sim 8 \times 10^{-11}$Torr pressures.

1. Introduction

The ability to trap individual isolated ions provides an opportunity to experimentally test the foundations of quantum mechanics. Observation of quantum jumps [1, 2] for a single ion using the Dehmelt shelving scheme [3] yield a means of testing, with a single resettable degree of freedom, on the inherent randomness of quantum mechanics [4, 5, 6]. An investigation of the consequences of a purely quantum phenomena as quantum teleportation [7, 8], entanglement [9], especially as they relate to the goals of quantum computing has been facilitated by geometries where a larger number of ions can be trapped and stabilized.

In this paper a detailed description of the construction of the, vacuum system, imaging system, feedback loops, trap designs and laser systems needed to Doppler cool and trap a single strontium ion [10] are presented. In order to obtain greater control over the seeding of ions into the trap, 2 photon resonance enhanced photoionization is employed. For the technique presented both photons have identical energy (431nm) and the intermediate level is a virtual state. Both quadrupole [11] and linear traps are discussed. Linear traps have the advantage of minimizing micromotion when multiple ions are present [10, 12].

Two particle entangled states have been realized in both cavity QED [13] and in ion traps [14]. In cavity QED information is transferred between the electronic states of various atoms via the modes of the cavity. Challenges presented to this approach include, the short confinement times and the need to achieve high Q (so that the decoherence time is sufficiently long until the conditional dynamics is performed) [15]. In a ion trap containing multiple ions, the motional quantum levels are determined by the potential well as modified by the mutual coulomb interaction. These ladder states then serve as a memory for quantum information. The difficulty then is the achievement of a joint motional ground state and the problem with heating of the ions.

A goal of this research effort is to combine the control facilitated by ion traps with the virtual excitation of a high-Q cavity [16] which is then used as bus for quantum memory, as already proposed and pursued by several groups [17, 18, 19].

2. Photoionization

In these experiments Strontium ions are efficiently created and fed into the trapping region via two-photon resonance-enhanced photoionization [20]. Compared to ionization via electron bombardment two photon resonance enhanced photoionization has various advantages. It's high efficiency means greatly reduced atomic flux, less electrode contamination and the elimination of problems due to charge accumulation on insulating surfaces, such as the distortion of trap potentials [21]. In addition the vacuum remains nearly unchanged during the process of loading the trap.

To ionize Sr a 431nm laser excites the transition $5s^2\ ^0S_0 \rightarrow (4d^2+5p^2)\ ^1D_2$, where the upper level is an autoionizing resonance that is $470cm^{-1}$ above the first ionization threshold (fig.1) [20]. The autoionizing state can also be reached with a two-step excitation using the intermediate $5s5p\ ^1P_1$ level. This approach requires two lasers at 461nm and 405nm and the absolute cross-section for transition from $5s5p\ ^1P_1$ to $(4d^2 + 5p^2)\ ^1D_2$ is $5.6{\times}10^{-15}cm^2$ [22]. In our scheme the ionization cross-section is $10^{-26}cm^4/W$ at the peak of the autoresonance. This is a theoretical estimate based on an R-matrix approach combined with the multichannel quantum defect theory (MQDT) [23]. The two-photon transition amplitude from the initial state $\psi_0(E_0)$ to the final $\psi_f(E_f = E_0 + 2\omega)$, using the lowest order in the perturbation theory is:

$$T_{fo}^{(2)} = \lim_{\eta \to 0+} \int \langle \psi_f | \mathbf{D}.\mathbf{e} | \varepsilon \rangle (E_0 + \omega - \varepsilon + i\eta)^{-1} \langle \varepsilon | \mathbf{D}.\mathbf{e} | \psi_0 \rangle$$

where $\mathbf{e}$ is the electric field polarization and $\mathbf{D}$ is the electric-dipole operator. The explicit summation over the discrete or continuum states is avoided using the Dalgarno-Lewis procedure [24]. The total cross section (in cm^4W^{-1}) is :

$$\sigma' = \sigma/I = 5.7466 \times 10^{-35} \sum_j |T_{fo}^{(2)}|^2$$

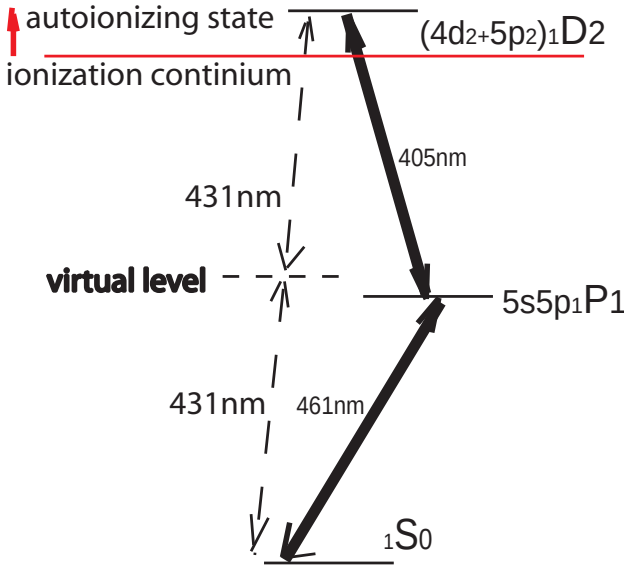

FIG. 1: Relevant level diagram of neutral Strontium used for the photoionization method. In this work the 431nm light is supplied by a 100fs, 0.5W average power pulses of a doubled TiSapphire laser.

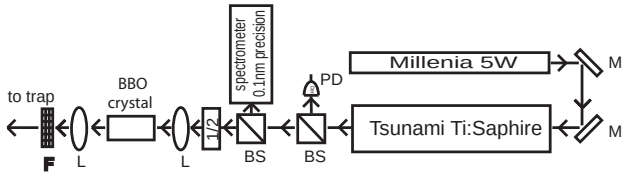

FIG. 2: Photoionizing system at 431nm.

where I is the laser intensity (in Wcm^{-2}) and the sum is performed over the possible total angular momentum states allowed by the Wigner-Echart theorem. In our case the laser is linearly polarized so both the $J = 0$ and $J = 2$ final states can be reached.

The setup is shown on figure 2. A Tsunami laser (Spectra-Physics) is used to provide 100fsec pulses at 82Mhz. The average power is ∼1/2W and the spectral width is ∼6nm. The output at 862nm is doubled with a BBO (2mm) crystal in a single pass giving 50mW of average power at 431nm. The beam is then expanded with a bi-concave lens (f=-3cm) and then focused in the trap region by a bi-convex lens (f=15cm). The focal width is $2\omega_0$=20μm. The photoionization probability per pulse [25]is

$$P_{ion} = (I^2\sigma'/\hbar\omega)\tau$$

where τ is the pulse length, 100fsec. So an estimate of the rate of photoionization averaged over the volume defined by the focal width of the beam and the length L of the trapping volume (which is smaller than the Rayleigh length) is calculated by averaging over the thermal trajectories of background atoms as they transverse the interaction volume to obtain

$$R_{ion} = P_{ion}(n_0\omega_0/8T)(2\pi\omega_0 L)$$

where n_0 is the atomic density and T is the time between 2 consecutive pulses. For a typical oven temperatures the pressure of the Sr vapor is 10^{-9}Torr which gives a estimate of $R_{ion} \approx 10sec^{-1}$.

In separate "proof of principle" experiment the 431nm output beam was focused 5mm from the aperture of a small Sr oven in a vacuum chamber. Under the point where the atomic beam and the laser beam meet (2cm away) a electron multiplier(EM) was positioned to detect the ionised Sr atoms. The EM was biased to $-2000V$ relative to a mesh 1cm above the photoionization region. The observed counting rate (fig.3) was consistent with theoretical predictions.

3. Laser systems for Sr^+

We constructed 4 laser systems required for driving the transitions in the "N-level" structure shown on fig.4.

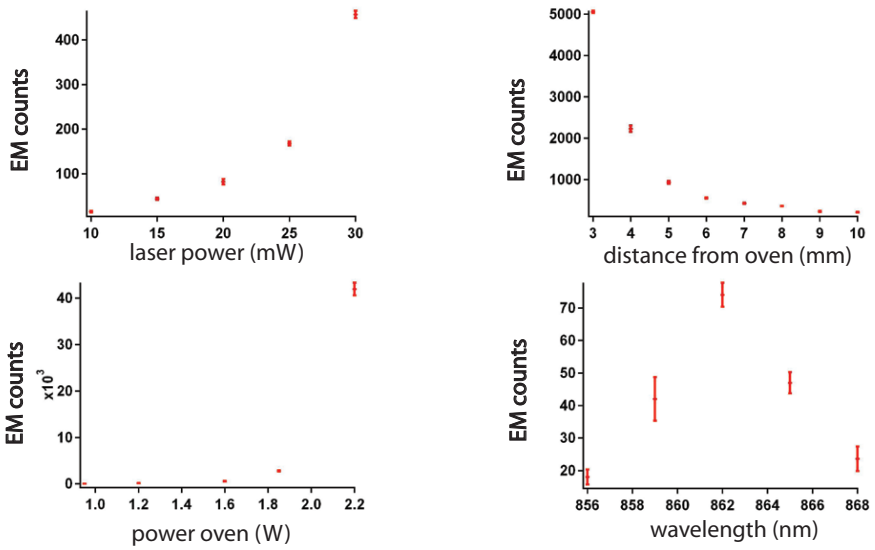

FIG. 3: Electron multiplier counts per second (used here instead of arbitrary units) as a function of laser detuning, atomic oven power, laser power and distance between the laser focal spot and atomic oven aperture.

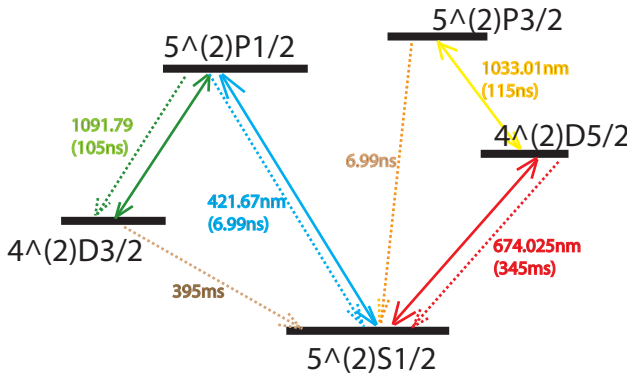

FIG. 4: Relevant levels structure.

The laser at 422nm (fig.5) [26] excites the $S_{1/2} \leftrightarrows P_{1/2}$ cooling transition. It has a short life time of $7.87sec$ and its fluorescence facilitates visual detection of even a single trapped ion. The heart of this laser system and also the one at 674nm is the ECDL (extended cavity diode laser).

We constructed custom designed ECDl's in a Littrow configuration (fig.6) [27]. An antireflection coated laser diode (100mW) provides a diverging elliptical beam centered at ∼850nm, which then passes through an aspheric collimating lens (0.55 NA,f=4.5 mm), mounted in a tube. The collimated light then falls on a diffraction grating (1800 lines/mm), which couples about 20% of the light back to the laser diode and reflects 75% as a output. The whole structure lies on a modified mirror mount which is used for a rough adjustment of the diffraction grating. Precise positioning is provided by a PZT-stack mounted under one of the fine screws. The grating lies on a additional PZT piezoelectric transducer disk which is used to dynamically regulate the laser frequency based on an error signal (described below). A temperature sensor (10kΩ) is used to detect the temperature close to the diode and a Peltier thermoelectric cooler is used to keep the temperature stable to 1mK. The collimated beam next reflects from a mirror parallel to the grating so as to maintain a fixed output direction when the screw and the PZT stack are adjusted. The spectral width of such a ECDL is ∼1/2Mhz. The laser is encased in a 1/2 inch thick aluminum box and lies on a heavy steel brick on top of a 4 sorbothane padding which enhances vibration isolation.

The collimated 844nm beam coming from the ECDL is circularized with 2 prisms and then passes through 2 ∼30dB optical isolators. Next a bi-convex lens (f=150mm) is used to mode-match the beam into the doubling cavity and a $\lambda/2$ plate is used to rotate the polarization.

The triangular doubling cavity has 3 mirrors, a finesse of 60 and is 15cm on a side. The first mirror couples in the 844nm light with a 3% transmission efficiency (S-polarized light, at 844nm and at 30° angle of incidence), which is

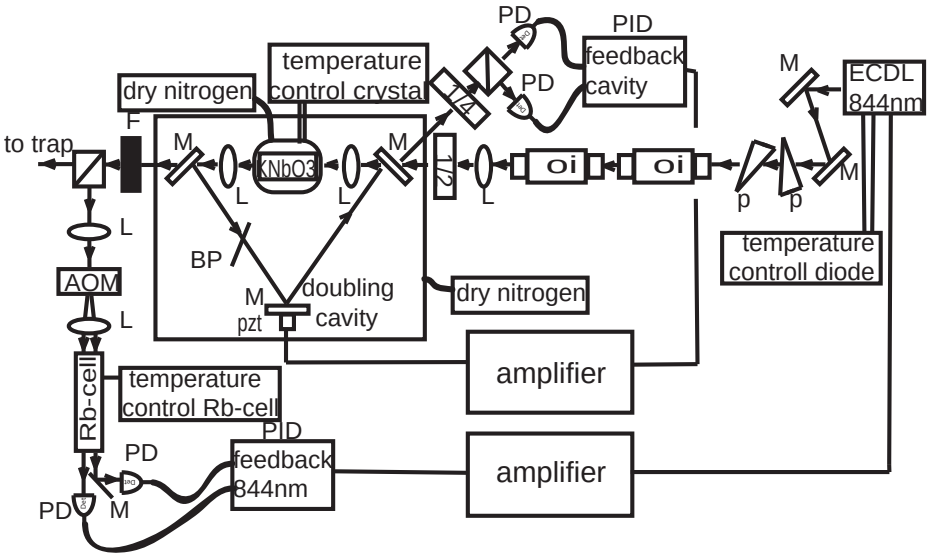

FIG. 5: 422nm laser system for Doppler cooling driving the $S_{1/2} \leftrightarrows P_{1/2}$ transition [26].

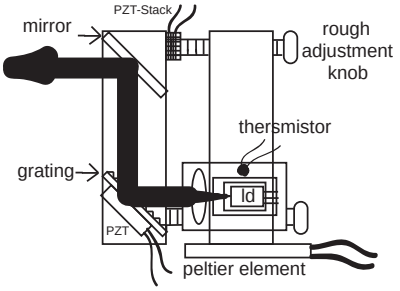

FIG. 6: Extended-cavity diode laser.

chosen to match the losses per turn in the cavity. The second mirror is the output coupler which for S-polarized light reflects >99.8%, at 30°, for 844nm and for P-polarized light transmits >80% at 30° angle of incidence for 422nm. The third mirror is simply a reflector >99.9% for 844nm, S-polarized light, at 30° angle of incidence. A PZT-stack is positioned behind that mirror to provide feedback and keep the cavity locked to the 844nm laser (details below). A 1cm antireflection-coated $KNbO_3$ crystal is positioned halfway between, the input and output couplers, as well as 2 bi-convex lenses (f=50mm, antireflection coated for 844nm). The lenses form a tight focus in the crystal, with Rayleigh length on the order of the crystal's length so as to efficiently generate the second harmonic [28]. The crystal is noncritically, type I phasematched at $-17°$ Celsius. Temperature is detected close to the crystal with AD590 sensor and is controlled, to 1mK precision with a Peltier element. The crystal, the Peltier element and copper heat sink (with a running chilled water) are in a acrylic chamber vented with dry nitrogen so as to, prevent freezing, preserve the antireflection coating and cavity finesse. The acrylic chamber is vented directly out of the cavity so as to avoid thermally driven changes in geometry. The doubling cavity also has a polarizing plate positioned at Brewsters angle which transmits only that light which is polarized parallel to the a-axis of the crystal. It is also a part of a modulation free method for stabilizing the cavity [29]. This method is based on the measurement of the ellipticity of the light reflected from the input coupler. It uses a $\lambda/4$ plate, a polarizing beamsplitter with an axis at 45° relative to the $\lambda/4$ plate and 2 photodiodes. The difference voltage generates an error signal which is then fed into the PZT-stack of the cavity. When the cavity contains a standing wave, which maximizes the pump (844nm)power in the crystal, the polarization of the light reflected from the input coupler is rotated from the polarization of the incoming 844nm light (but it is still linearly polarized). In this situation the 2 photodiodes detect equal signal. When any disturbance drifts the cavity away from resonance the reflected light is elliptically polarized and an error signal is created. The doubling system is enclosed in a sealed aluminum box and rests on sorbothane padding.

Approximately $80\mu W$ at 422nm are produced from the enhancement cavity; 95% is directed into the trap and 5%

is used to generate an absolute reference for the laser system [26]. This stage begins with a blue pass filter (which eliminates the residue of $844nm$ light)and a f=150mm lens which focuses the light into an acousto-optic modulator. The AOM produces frequency downshifted and unshifted beams of similar power. The beams are collimated by a f=50mm lens so as to traverse a 7.5cm long Rb cell, stabilized at $130°C$. The 2 beams are then detected by 2 photodiodes. The Doppler-broadened absorption profile of the Rubidium vapor consists of 3 gaussian due to the natural mixture of ^{85}Rb and ^{87}Rb. The central gaussian is closest to the center of the $^{88}Sr^{+}$ $5s^2S_{1/2} \rightarrow 5p^2P_{1/2}$ transition (with a peak absorption ∼500Mhz lower than the targeted Sr transition). The width of the Rb absorption profile is ∼1.3Ghz. The down-shifted beam falls on the other side of the gaussian thus making the error signal (the difference of the signals of the 2 diodes) less sensitive to temperature drifts of the Rb cell and power drifts of the $422nm$ beam.

To trigger the clock transition (fig.4) $S_{1/2} \leftrightarrows D_{5/2}$ a 674nm laser is needed (fig.7). This is a very narrow transition with lifetime 1/3sec which can be used to excite quantum jumps. It can also play the role of a "quantum bit", or serve as the analog of a spin up $|\uparrow\rangle$ and spin down $|\downarrow\rangle$ states of a spin 1/2 particle. This is the most demanding laser

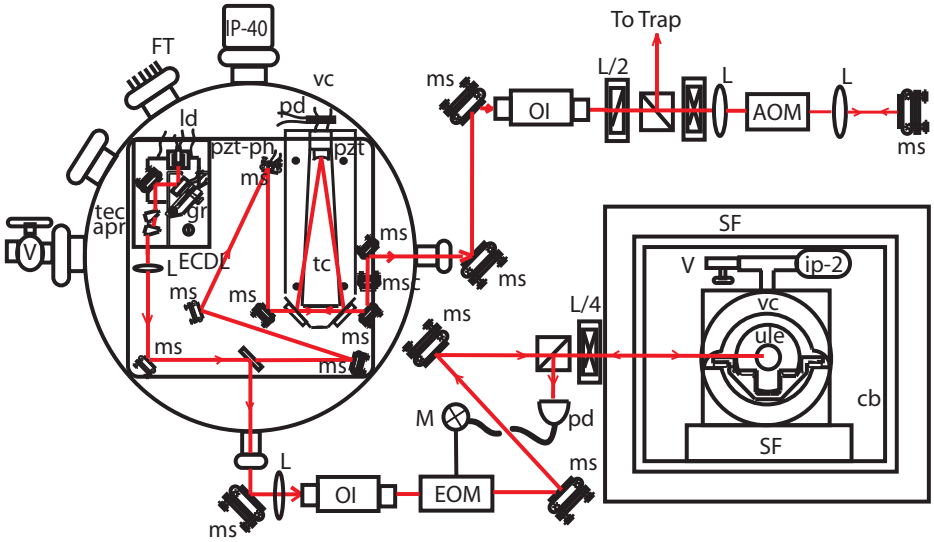

FIG. 7: Laser system for 674nm. $5^2S1/2 \rightleftarrows 4^2D5/2$ Strontium transition. The abbreviations used are: IP-ion pump, FT-feedthrough, V-valve, VC-vacuum chamber, tc-triangular cavity, ms-mechanical stages, pd-photodiode, pzt-piezoelectric crystal, apr-anamorphic prisms, tec-Peltier element, kn-precision knob, msc-optical coupler, OI-optical isolator, L/2-halfwave plate, L/4-quarter wave plate, L-lens, AOM-aqcousto-optic modulator, EOM- electrooptic-modulator, PD-avalanche photodiode, M-mixer, SF-sterofoam isolation, cb-copper cage, ULE-Ulrta-low expansion cavity

system employed in the Strontium ion trapping experiment. The spectral width of the laser is decreased to less than 10KHz in several stages.

In the first stage the single antireflection coated diode at 670nm is placed in an ECDL (Extended Cavity Diode Laser) setup which is similar to the one used in the 422nm Doppler cooling laser system. Now however, the whole body of the ECDL including the mechanical stages are made from Super-Invar (thermal expansion $0.6 \times 10^{-6}(°C)^{-1}$). The temperature of the ECDL is controlled to long-term stability of 1mK with a peltier element. After leaving the ECDL the beam with a spectral width of $1Mhz$ is circularized with 2 prisms. In the second stage the beam is mode-matched with a single lens to the TEM_{00} mode of a triangular Fabri-Perot cavity with a FSR of 1Ghz and finesse of 200. Most of the designs implementing an optical feedback from a external cavity take the output before the cavity and need to adjust the cavity position so the first reflection from the input coupler doesn't couple back to the diode but the leakage beam does. This requires either a 2 mirror cavity in a almost confocal arrangement with slight misalignment or a triangular cavity which should be adjusted to couple back the leakage beam and to resonate at the same time [30]. In the design that we are using the optical feedback comes from a small 4% reflective plate positioned after the output of the triangular cavity, which allows the cavity to be aligned and the optical feedback to be adjusted separately [31]. Another advantage of this design is that the output is taken in transmission of the triangular cavity so additional filtering is applied to the broad fluorescent background of the diode existing even after the optical feedback is applied. At the sharp angle of the triangular cavity there is a high reflector with a curvature R=75cm, chosen so the higher modes of the cavity are pushed away from the TEM_{00} mode. Behind the reflector, which is mounted on a tubular pzt-stack a small photodiode detects the leakage from the reflector (fig.8). The path

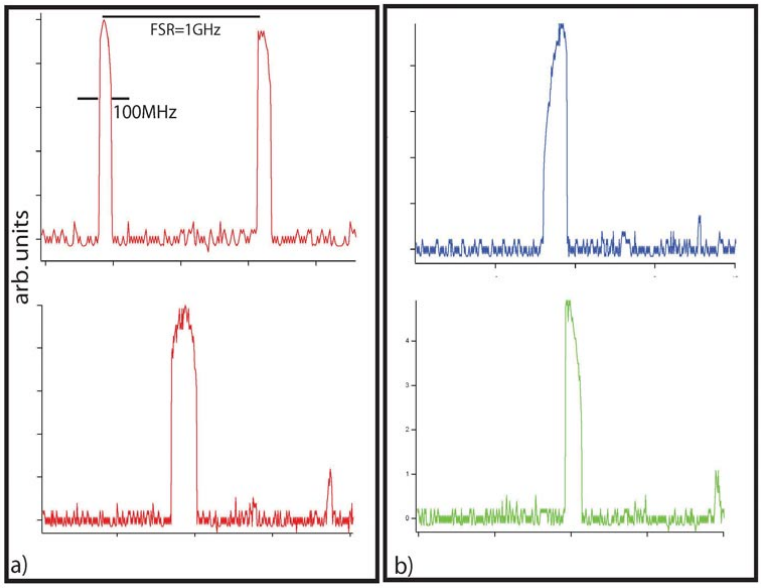

FIG. 8: Triangular cavity transmission a)cavity-pzt swept and optical feedback path on resonance b)optical feedback out of resonance, the peaks are asymetric.

from the triangular cavity and the laser diode has to be adjusted so that the feedback beam and the outgoing one are in phase. For that purpose one of the reflectors guiding the beam between the ECDL and the cavity is glued on a pzt-stack (called pzt-ph on fig.7) When the optical feedback is on the ECDL follows the cavity over a range of about 100Mhz (fig.8). Narrowing of the laser linewidth relative to the ECDL is then given by [32]:

$$\Delta\nu = \frac{\Delta\nu_{ecdl}}{\beta(\frac{L_p}{L_{ecdl}}\frac{F_{tc}}{F_{ecdl}})^2}$$

where L_p and L_{ecdl} are the ECDL and cavity lengths and F_{tc} and F_{ecdl} are the ECDL and cavity finesses. Linewidth narrowing is given as the square of the ratio between the HWHM of the triangular cavity transmission fringes (fig.8) with and without optical feedback. We estimate that after the triangular cavity the laser linewidth is $< 10kHz$.

The first and most important part of the laser system consisting of ECDL, triangular cavity and reflectors guiding the beam between the two is laid on a Super-Invar plate (8"x8"x1"), which is then positioned in a custom made UHV chamber (fig.7) held at $10^{-7}Torr$ only by a Starcell 40L/s ion pump. The super-invar plate lies on 4 viton o-rings and the whole vacuum chamber together with the ion pump sits on 2 stages of sorbothane padding in order to achieve sufficient vibration isolation.

From the vacuum chamber the output in transmission of the triangular cavity which is spatially and spectrally filtered (even when the laser is narrowed from the optical feedback there is a broad fluorescent background from the laser diode) to send to the ion trap. To tune the beam across the Sr transition without deflecting the beam, we employ a double pass through a Acousto-optic modulator (Brimrose GPF-600-400).

A small fraction of the beam coming from the ECDL (about $60\mu W$) is deviated before reaching the triangular cavity and sent to a Ultra-low expansion cavity (ATfilms high grade Corning glass, 2×10^5 Finesse, 10cm length). The cavity is held in vacuum $10^{-7}Torr$ in a temperature controlled custom made UHV chamber with a 2L/s ion pump acting on it. The vacuum chamber is then enclosed in a 1/4" thick copper box, temperature controlled with a nichrome heater wire to 2mK at $25°C$(which is approximately the zero crossing temperature of the thermal expansion coefficient of the Corning ULE cavity). The copper box is further isolated from the room environment with a 1.5" thick styrofoam wall with small holes left only for the laser beams. The goal is to stabilize the ULE cavity temperature to $< 10\mu K$.

We intend to use Drever-Pound-Hall(DPH) method to lock the laser to the ULE cavity. To create a DPH error signal we modulate the laser phase with an Electro-optic modulator (New Focus) at 20Mhz. The error signal is detected in reflection (fig.7). The self-constructed Servo circuit used for feedback has a proportional gain of 0.5 and a integral gain of $10^6 s^{-1}$. We intend to feed this signal to the injection current of the laser diode and a filtered slow component will be fed to the triangular cavity pzt.

When the triangular cavity and the path between the triangular cavity and the ECDL are at resonance, so the transmission fringe looks like the bottom left part of fig.8,it takes an hour to observe a change bigger than 1% even in the absence of a electronic lock . Such a lock has been implemented by dithering the "phase-pzt" to obtain

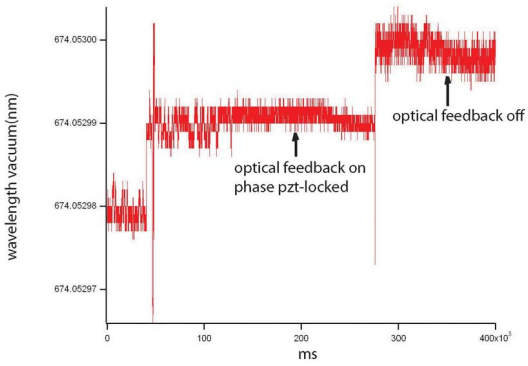

FIG. 9: Triangular cavity transmission a)cavity on resonance and optical feedback path on resonance b)optical feedback off, spectral linewidth determined just by the ECDL.

transmission as a function of path length near the maximum. Derivatives of this signal determine the symmetry of the transmission peak. Feedback to the same "phase-pzt" then locks it to the path length that achieves symmetric transmission. The effect of this feedback control as recorded by the wavemeter is shown on fig.9.

For more reliable long term stability and even narrower laser linewidth we will need the lock to the ULE cavity fringe although the performance at that stage is already suitable for sideband cooling experiments.

To amplify the rate of sideband cooling, which will otherwise rely on the spontaneous decay of the $4^2D_{5/2}$ transition (1/3sec.) we built a laser at 1033nm which can open the $4^2D_{5/2} \leftrightarrows 5^2P_{3/2}$ transition which has a short lifetime of 7ns down to the ground state. The 1033nm laser is a ECDL without an absolute reference but with good temperature control, vibration isolation and choice of materials (super-invar). It stays within 3Mhz for 1 hour, which is well within the transition bandwidth.

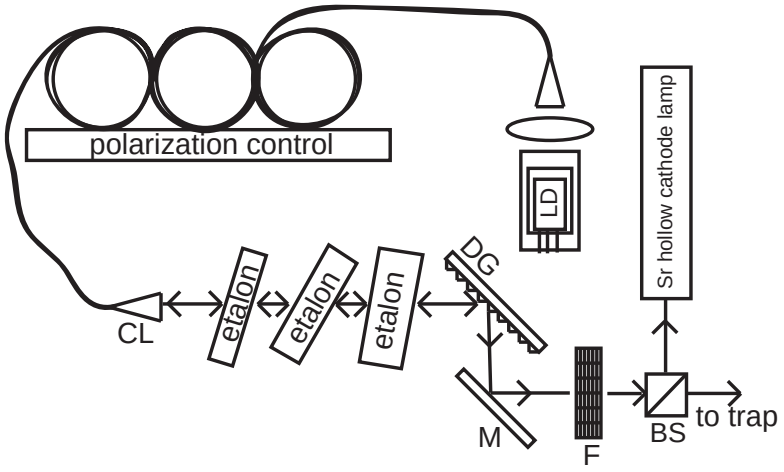

FIG. 10: 1092nm laser system driving the $P_{1/2} \leftrightarrows D_{3/2}$ transition.

Unfortunately an ideal V-level structure in Sr doesn't exist and one in 13 decays of the $P_{1/2}$ level falls into the $D_{3/2}$ state, so that laser cooling and fluorescence are interrupted. To optically pump the ions out of the $D_{3/2}$ level a laser at 1092nm is needed. We use a specially made Nd^{3+}-doped fiber (fig.10) [33] laser. It is pumped by a 150mW laser diode at 830nm and it emits between 1060nm and 1100nm. The fiber core has 5% germania by eight containing Nd^{3+}-doped ions at circa 500-1000ppm and absorption is 3.5dB/m @ 830nm. The fiber (3m long) is positioned between a input coupler which is antireflection coated at 780-850nm range and is >99.9% reflective for 1060-1100nm. One end of the fiber is contacted with the input coupler and on the other end outgoing light is collimated to a 1mm beam which travels ∼20cm before reaching the grating (1200lines/mm) positioned at a littrow angle to roughly select the needed wavelength. About ∼50% of the light returns back to the cavity. Between the collimator and the grating there are 3 uncoated etalons (1mm,5mm and 15mm thick) which are used to further narrow the laser linewidth and for fine tuning. The full spectral width is 1Ghz and the tuning range is from 1070nm to 1100nm. The desired wavelength,

1091.79nm can be simply dialed up on a wave meter, or found by exciting an optogalvanic effect in a Sr hollow cathode lamp. Active feedback is not needed because the spectral structure of the laser consists of several modes spaced 40Mhz apart (corresponding to the length of the cavity) and each one of them has enough power (total power is 5mW) to saturate the transition. During the time of the experiment the laser never drifts so dramatically to leave the transition out of it's 1Ghz spectral width. Finally the 1092nm beam is overlapped with the 422nm and 674nm beams. The 431nm beam for the photoionization is separate and perpendicular to the other three. All the beams lie perpendicularly to the direction of observation.

4. Vacuum system

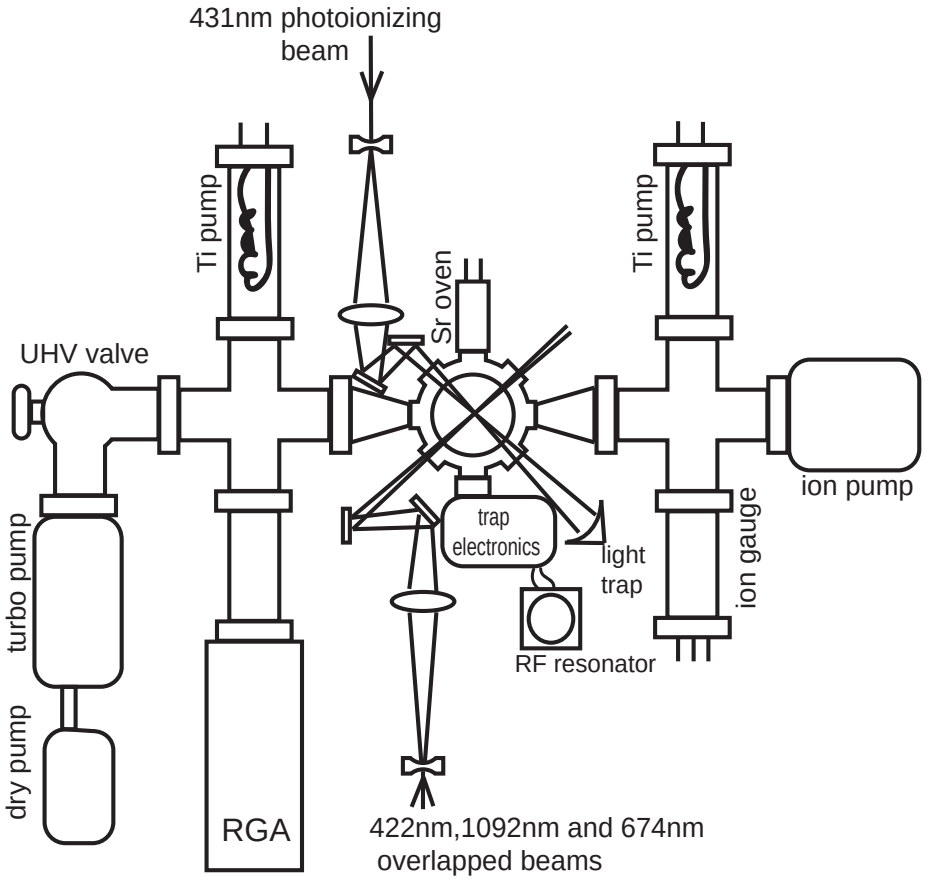

FIG. 11: Vacuum system and focusing optics.

The vacuum system is shown in fig.11. The ion trap is positioned in the middle of a commercially available octagon with 2 (4.5inch) view ports used for detection of the ion fluorescence and 8 (1.33inch) small ports used one for, electrical feedthrough, the Sr oven, the overlapped 422nm, 674nm and 1092nm beams, the 431nm photoionizing beam and pumping.

The pressure, typically 8×10^{-11} Torr is achieved in several stages. First the range of 2×10^{-8} is achieved by a turbo pump (20l/s), backed up by a diaphragm rough pump (capable of achieving 1-2Torr). The whole system is baked in place for 24 hours at $150°C$(the only exception being the ion pump baked to $250°C$) after each time the chamber has been opened to atmosphere. Prior to the assembly, all steel components are baked at $450°C$ under vacuum for more than 1 weeks in order to minimize the hydrogen content, which is the factor that determines the lowest achievable pressure.

In the second stage 2 titanium filaments are flashed for about 1min with 50Amps of AC current to evaporate a titanium layer on the walls of the cylinders that surround the filaments. This reactive layer efficiently removes all the getterable gasses. The noble gases are pumped by a 20l/s ion Starcell pump. At this point a UHV valve is closed to separate the turbo pump from the rest of the experiment and only the titanium and ion pumps act on the chamber. The turbo and rough pumps are now switched off and pressure is monitored by an RGA and an ion gauge.

5. Imaging system

The imaging system (fig.12A) consists of a 28mm camera lens positioned above the top 4.5inch vacuum port. It

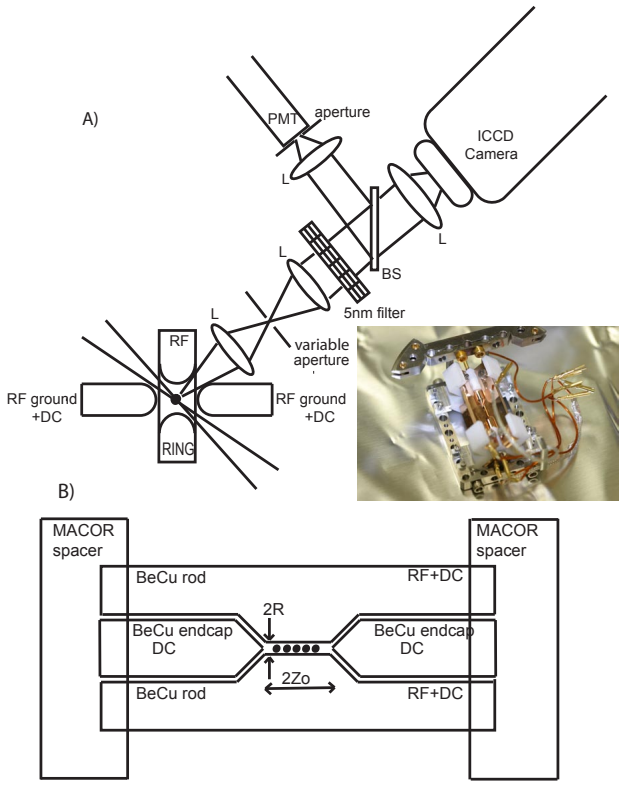

FIG. 12: a) Quadrupole Paul trap and imaging system b) Linear trap (the same imaging system used).

creates a (1:1) image 5cm above the port. In the plane of the image an adjustable rectangular aperture (consisting of 4 independently translatable blades)is used to select the signal and suppress scattered light (which is especially strong from the electrodes). Next, the fluorescent light is collimated by a 28mm camera lens and then refocused on the photocathode of a ICCD camera by a 200mm camera lenses. In between the 2 lenses there is a laser line filter centered at 422nm with width of 5nm. Also there is a 50/50 pellicle nonpolarised beamsplitter which deflects half of the collimated light onto a bi-convex lens (f=50mm), which focuses it onto a PMT tube. Such an arrangement allows for simultaneous observation of the ions with the camera and photon counting with the PMT.

6. Different Ion Traps

Fig.12a,b shows various ion traps that were built. We started with a standard Paul trap [11, 34] with characteristic endcap distance $2z_0$=2mm (fig.8a). With this trap we used an iridium filament electron gun for ionization. The filament was biased at -40V relative to the endcaps and was positioned 7.5mm away from the trapping region. With 3Amps running through the filament about 0.1μA of electron current crossed the trap. The trap itself was made out of stainless steel 304. The only non-conducting component was made from Macor and carefully screened. It was used to insulate the ring of the trap on which the RF=300Vpp at 7Mhz was applied. On the other side of the trap 1.5cm away, opposite to the e-gun a tantalum oven with several 1mm pieces of Sr was positioned. The oven has 1mm aperture and care is taken to make sure that the atomic flux crosses the region of the trap.

We also built a linear trap(fig.12b) [12]. The distance between the endcaps is $2z_0$=6mm and the distance from the trap axis to the rod surface is R=0.75mm. The trap was machined out of Beryllium-Copper 172 alloy and the spacers were made from Macor as shown. With this trap we used photoionization (not the electron gun), so the exposed insulators were of less concern. Nevertheless the trap region doesn't directly "see" any insulating surface. The electrode surfaces were polished with 100nm grit diamond paste and then were chemically cleaned with sulphuric acid and hydrogen peroxide solution. The RF potential for both types of traps is provided by a quarter-wave helical resonator [35] (Q=60) made out of copper with one secondary coil for the quadrupole Paul trap. For the linear trap 2 secondary coils provide the opportunity for separate DC offsets, which are used for compensation of the potential imperfections and to minimize micromotion of the ions. Separate DC potentials can also be applied to the endcaps and to the other side-rods that are at RF ground. Just outside the vacuum the DC electrodes are connected to ground with 0.1μF to reduce the inductively coupled RF noise.

6. System performance

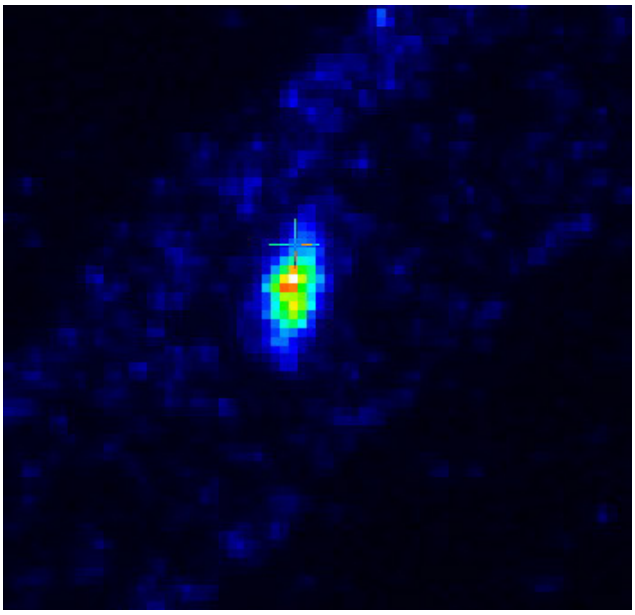

FIG. 13: Linear trap. A string of ions is formed in the trap. The ions are visible one at a time due to the tight focus. Pixel size 5x5μm.

During an experimental run we first [10] slowly lower the temperature of the $KNbO_3$ crystal (to prevent crack of the coating) until it reaches roughly $-17^{\circ}C$. During this time the temperature controllers for the ECDL's of the 422nm, 674nm laser and the Rb-cell are switched on. Thermal equilibrium is reached within 1/2 hour. At this point all the 4 lasers are on with the light at 431nm being too weak to excite ionization, because the laser at 862nm is out of lock.

To optimize the performance of the doubling cavity its PZT is pulsed at 10Hz and the transmission peaks at 844nm are observed on a removable photodiode. By adjusting the cavity components its finesse is maximized. At this point the diode is removed and the cavity is locked to the 844nm laser. Now the 2 beams at 422nm, 1092 nm are sent to the wavemeter and their wavelengths are adjusted by tilting the ECDL's cavities via the PZT-stacks. By sweeping the wavelength of the 422nm laser we can map out the absorbtion profile of the Rb vapor and lock the 844nm ECDL to its proper location. The RF potential is switched on to 300Vpp and the DC potential on the endcaps is adjusted at 50V. The Sr oven has by now been preheated for about 2 hours with$\sim$1.5Amps DC current. The oven current is now increased to 2.5Amps and simultaneously the 431nm output is fired up as the 862nm laser is modelocked. Several amps running through a small coil under the vacuum chamber generate a magnetic field of several gauss which prevents the ions from being driven into a dark state [36].

After several seconds a small cloud is visible on the ICCD camera and both the ionizing laser and the oven are switched off. Now we gradually decrease the RF and the DC on the endcaps until most of the ions escape the trap. The remaining ions form a stable linear string (for the linear trap) that can live many hours (fig.13).

7. Acknowledgments

It is a pleasure to thank Alan Madej and Pierre Dube(National research council of Canada) and Robert Scholten(University of Melbourne) for the numerous very helpful advices on the fabrication of the laser systems. Ralph Wuerker , Dana Berkeland (LANL) and Nan Yu (JPL) for experimental suggestions and recommendations on the whole experiment, Brian Naranjo (UCLA, Physics department) for providing his help and knowledge for the vacuum system construction, Makan Mohageg(UCLA,JPL) for advises on the PID circuits and Alex Bass (UCLA, Physics department) for providing deep theoretical ideas on fundamental physics questions which was rather encouraging. Research supported in part by Darpa and the ONR, and a gift from the Elwood and Stephanie Norris Foundation.

[1] W. Nagourney, J. Sandberg, and H. Dehmelt, Phys. Rev. Lett. **56**, 2797 (1986).
[2] J. C. Bergquist, R. G. Hulet, W. M. Itano, and D. J. Wineland, Phys. Rev. Lett. **57**, 1699 (1986).
[3] H.J.Dehmelt, Bull.Am.Phys.Soc. **20**, 60 (1975).

[4] T.Erber and S. Putterman, Nature **318**, 41 (1985).
[5] T.Erber, P.Hammerling, G.Hochney, M.Porrati, and S.Putterman, Ann.Phys. **190**, 254 (1989).
[6] D. J. Berkeland, D. A. Raymondson, and V. M. Tassin, Physical Review A (Atomic, Molecular, and Optical Physics) **69**, 052103 (pages 4) (2004), URL http://link.aps.org/abstract/PRA/v69/e052103.
[7] C. H. Bennett, G. Brassard, C. Crépeau, R. Jozsa, A. Peres, and W. K. Wootters, Phys. Rev. Lett. **70**, 1895 (1993).
[8] A.Furusawa, J. andS.Braunstein, C.Fuchs, H.J.Kimble, and E.Polzik, Science **282**, 706 (1998).
[9] Q. A. Turchette, C. S. Wood, B. E. King, C. J. Myatt, D. Leibfried, W. M. Itano, C. Monroe, and D. J. Wineland, Phys. Rev. Lett. **81**, 3631 (1998).
[10] D. J. Berkeland, Rev. Sci. Instrum. **73**, 2856 (2002), URL http://link.aip.org/link/?RSI/73/2856/1.
[11] R. F. Wuerker, H. Shelton, and R. V. Langmuir, Journal of Applied Physics **30**, 342 (1959), URL http://link.aip.org/link/?JAP/30/342/1.
[12] M. G. Raizen, J. M. Gilligan, J. C. Bergquist, W. M. Itano, and D. J. Wineland, Phys. Rev. A **45**, 6493 (1992).
[13] E. Hagley, X. Maître, G. Nogues, C. Wunderlich, M. Brune, J. M. Raimond, and S. Haroche, Phys. Rev. Lett. **79**, 1 (1997).
[14] Q. A. Turchette, C. S. Wood, B. E. King, C. J. Myatt, D. Leibfried, W. M. Itano, C. Monroe, and D. J. Wineland, Phys. Rev. Lett. **81**, 3631 (1998).
[15] G. Rempe, R. J. Thompson, H. J. Kimble, and R. Lalezari, Opt. Lett. **17**, 363 (1992).
[16] S.-B. Zheng and G.-C. Guo, Phys. Rev. Lett. **85**, 2392 (2000).
[17] G. R. Guthhrlein, M. Keller, K. Hayasaka, W. Lange, and H. Walther, Letters to Nature **414**, 49 (2001).
[18] A. Kreuter, C. Becher, G. P. T. Lancaster, A. B. Mundt, C. Russo, H. Häffner, C. Roos, J. Eschner, F. Schmidt-Kaler, and R. Blatt, Physical Review Letters **92**, 203002 (pages 4) (2004), URL http://link.aps.org/abstract/PRL/v92/e203002.
[19] A. Mundt, A. Kreuter, C. Russo, C. Becher, and D. L. J. E. F. S.-K. R. Blatt, Appl. Phys. B **76**, 117 (2003).
[20] M. A. Baig, M. Yaseen, R. Ali, A. Nadeem, and S. A. Bhatti, Chem. Phys. Lett. **296**, 403 (6 November 1998), URL http://www.ingentaconnect.com/content/els/00092614/1998/00000296/00000003/art01059.
[21] N.Kjaergaard, L.Hornekaer, A.M.Thommesen, Z.Videsotopesen, and M.Drewsen, Appl. Phys. B: Lasers and Optics **71**, 207 (2000), URL http://dx.doi.org/10.1007/s003400000296.
[22] W. Mende, K. Bartschat, and M. Kock, J. Phys. B: At. Mol. Opt. Phys. **28**, 2385 (1995).
[23] E. Luc-Koenig, M. Aymar, J.-M. Lecomte, and A. Lyras, J. Phys. B: At. Mol. Opt. Phys. **31**, 727 (1998).
[24] A.Dalgarno and J. T. Lewis, Proc. R. Soc. A **233**, 70 (1955).
[25] L. Deslauriers, M. Acton, B. B. Blinov, K.-A. Brickman, P. C. Haljan, W. K. Hensinger, D. Hucul, S. Katnik, J. R. N. Kohn, P. J. Lee, et al., Physical Review A (Atomic, Molecular, and Optical Physics) **74**, 063421 (pages 10) (2006), URL http://link.aps.org/abstract/PRA/v74/e063421.
[26] A. Madej, L.Marmet, and J. Bernard, Appl. Phys. B: Lasers and Optics **67**, 229 (1998), URL http://www.springerlink.com/content/13puqr5nt51au74j.
[27] C. J. Hawthorn, K. P. Weber, and R. E. Scholten, Review of Scientific Instruments **72**, 4477 (2001), URL http://link.aip.org/link/?RSI/72/4477/1.
[28] M. K. Chun, L. Goldberg, and J. F. Weller, Applied Physics Letters **53**, 1170 (1988), URL http://link.aip.org/link/?APL/53/1170/1.
[29] T. W. Hansch and B. Couillaud, Opt. Commun. **35**, 441 (1980).
[30] D.Schnier and A. Madej, Opt. Commun. **105**, 388 (1994).
[31] J.Labaziewicz, P. Richerme, K. Brown, I.Chuang, and K. Hayasaka, Opt. Lett. **32**, 572 (2007).
[32] P.Laurent, A. Clairon, and C.Breant, IEEE J. Quantum Electron. **25**, 1131 (1989).
[33] A. Madej, W.E.Berger, G.R.Hanes, and M.S.O'Sullivan, Opt. Commun. **73**, 147 (1989).
[34] W. Paul, Rev. Mod. Phys. **62**, 531 (1990).
[35] W. W. Macaplin and R. O. Schildknecht, Proc. IRE **47**, 2099 (1959).
[36] D. J. Berkeland and M. G. Boshier, Phys. Rev. A **65**, 033413 (2002).